

# Power sensor characterization from 110 GHz to 170 GHz using a waveguide calorimeter

Celep, Murat; Salek, Milan; Stokes, Daniel; Skinner, James; Wang, Yi

DOI:

[10.1109/TIM.2022.3144209](https://doi.org/10.1109/TIM.2022.3144209)

License:

Other (please specify with Rights Statement)

*Document Version*

Peer reviewed version

*Citation for published version (Harvard):*

Celep, M, Salek, M, Stokes, D, Skinner, J & Wang, Y 2022, 'Power sensor characterization from 110 GHz to 170 GHz using a waveguide calorimeter', *IEEE Transactions on Instrumentation and Measurement*, vol. 71, 9684391. <https://doi.org/10.1109/TIM.2022.3144209>

[Link to publication on Research at Birmingham portal](#)

## **Publisher Rights Statement:**

M. Celep, M. Salek, D. Stokes, J. Skinner and Y. Wang, "Power Sensor Characterization from 110 GHz to 170 GHz using a Waveguide Calorimeter," in *IEEE Transactions on Instrumentation and Measurement*, doi: 10.1109/TIM.2022.3144209.

© 2021 IEEE. Personal use of this material is permitted. Permission from IEEE must be obtained for all other uses, in any current or future media, including reprinting/republishing this material for advertising or promotional purposes, creating new collective works, for resale or redistribution to servers or lists, or reuse of any copyrighted component of this work in other works.

## **General rights**

Unless a licence is specified above, all rights (including copyright and moral rights) in this document are retained by the authors and/or the copyright holders. The express permission of the copyright holder must be obtained for any use of this material other than for purposes permitted by law.

- Users may freely distribute the URL that is used to identify this publication.
- Users may download and/or print one copy of the publication from the University of Birmingham research portal for the purpose of private study or non-commercial research.
- User may use extracts from the document in line with the concept of 'fair dealing' under the Copyright, Designs and Patents Act 1988 (?)
- Users may not further distribute the material nor use it for the purposes of commercial gain.

Where a licence is displayed above, please note the terms and conditions of the licence govern your use of this document.

When citing, please reference the published version.

## **Take down policy**

While the University of Birmingham exercises care and attention in making items available there are rare occasions when an item has been uploaded in error or has been deemed to be commercially or otherwise sensitive.

If you believe that this is the case for this document, please contact [UBIRA@lists.bham.ac.uk](mailto:UBIRA@lists.bham.ac.uk) providing details and we will remove access to the work immediately and investigate.

# Power Sensor Characterization from 110 GHz to 170 GHz using a Waveguide Calorimeter

Murat Celep, *Senior Member, IEEE*, Milan Salek, Daniel Stokes, *Member, IEEE*, James Skinner, Yi Wang, *Senior Member, IEEE*

**Abstract**—This paper proposes a new calorimetry-based measurement method to measure absolute microwave power obtained through DC substituted power from 110 GHz to 170 GHz (WG 29, WR 6/7 or D-band) using a custom-designed thin film microwave power sensor. This method complements traditional micro-calorimetry techniques used to provide traceability for microwave power in this band whilst diversifying the potential applications and accessibility to such traceability. The thermopile of the measurement system was characterized using a known DC power with the microwave sensor and the thermopile coefficient obtained. Absolute microwave power on the microwave sensor was calculated using the thermopile coefficient and was used to remove the effect of a thermal isolation section and calorimeter unbalance effect. To transfer the power traceability from the calorimeter to microwave power measurement applications, the effective efficiency of a device under test, consisting of a power sensor/meter combination was defined using the calorimeter’s absolute microwave power and the S-parameters of the measurement system and of the device under test. The effective efficiency of the device under test was obtained between 0.9386 and 0.9815 for the whole frequency band.

**Index Terms**— calibration, microwave sensor, calorimeter, microwave power, effective efficiency.

## I. INTRODUCTION

Traceability for microwave power in waveguides is most commonly obtained through the use of micro-calorimeter systems. However, it is also possible to modify these systems to allow their operation as a calorimeter as opposed to a micro-calorimeter system. The difference between these two types of systems is that a calorimeter is a characterizable terminating sensor which can be used to directly measure the incident absolute microwave power through thermal effects [1], [2]. Whilst a micro-calorimeter is an instrument that can be used to characterize different inserted terminating microwave transfer standards, which can then be subsequently used to measure microwave power [3] – [6].

The calorimeter technique relies on the measurement of temperature variations caused by DC or microwave power being dissipated on the DC load and microwave termination respectively. If the temperatures changes are equivalent for both

dissipated powers, then it can be inferred that the absolute dissipated DC and microwave powers are also equivalent. Therefore, this technique helps to define microwave power using DC substituted power.

There are many different types of terminating power sensors for low frequencies (below 110 GHz) on the market. However, most of them are not suitable for use with a micro-calorimeter system, instead requiring a separate transfer system and comparison method to propagate microwave power traceability. There is a subset of these commercial sensors which are suitable, typically thermistor or thermo-electric type sensors, but these are often difficult to obtain or not suitable for industrial applications. At higher frequencies (above 110 GHz), there are very few commercial options available for power sensors and none of them can operate within a micro-calorimeter system. The few commercial waveguide power sensor/meter combinations that are available above 110 GHz are typically calorimetric-type sensors, which operate using the same fundamental principles as their primary standard counterparts [7], [8]. Therefore, to perform micro-calorimeter measurements above this frequency, it is often necessary to custom-manufacture appropriate transfer standards [9], [10].

This paper proposes a new method using a modified micro-calorimeter to measure traceable absolute microwave power and to define an effective efficiency of a commercially available power sensor/meter combination as a device under test (DUT) for WG 29 (110 GHz to 170 GHz, WR 6/7 or D-band). The effective efficiency (EE) is defined as the ratio of the measured power ( $P_{DUT}$ ) as indicated by the DUT, to the known incident microwave power and is given as:

$$EE = \frac{P_{DUT}}{P_{inc}} \quad (1)$$

A custom thin-film bolometric-type microwave power sensor was used to modify a micro-calorimeter. The new measurement method using calorimetry methodology includes the characterization of the thin-film microwave power sensor in conjunction with a thermopile with known DC power. A short

This work was supported by the European Metrology Programme for Innovation and Research (EMPIR) Project 18SIB09 “Traceability for electrical measurements at millimetre-wave and terahertz frequencies for communications and electronics technologies”. The EMPIR Programme is co-financed by the participating states and from the European Union’s Horizon 2020 Research and Innovation Programme.

M. Celep, D. Stokes and J. Skinner are with National Physical Laboratory (NPL), Teddington TW11 0LW, U.K. (e-mail: murat.celep@npl.co.uk; daniel.stokes@npl.co.uk; james.skinner@npl.co.uk).

M. Salek and Y. Wang are with the Department of Electronic, Electrical and Systems Engineering, University of Birmingham, Birmingham B15 2TT, U.K. (e-mail: m.salek@bham.ac.uk; y.wang.1@bham.ac.uk).

foil method was used to remove the thermal isolation section effect.

In Section II, the theory of the modified calorimeter is given with newly derived equations and the characterization method described. Finally, measured system parameters, calculated microwave powers incident on the microwave and DUT sensors, and DUT effective efficiency are given in Sections III and IV.

## II. WG 29 BAND CALORIMETER

The waveguide calorimeter used in this work was originally designed as a micro-calorimeter for the 110 GHz – 170 GHz frequency band. This calorimeter has a similar design and structure except for the microwave sensor, to the micro-calorimeter described in [11] but in a higher frequency band. In order to adapt the micro-calorimeter design to function as a calorimeter, a microwave sensor is used to terminate the output of the thermal isolation section (TIS). Therefore, the measurement reference port is moved from the TIS output to the coupled arm of the directional coupler, usually used for the reference sensor in a micro-calorimeter measurement. The schematic for the layout of this waveguide calorimeter is illustrated in Fig. 1.

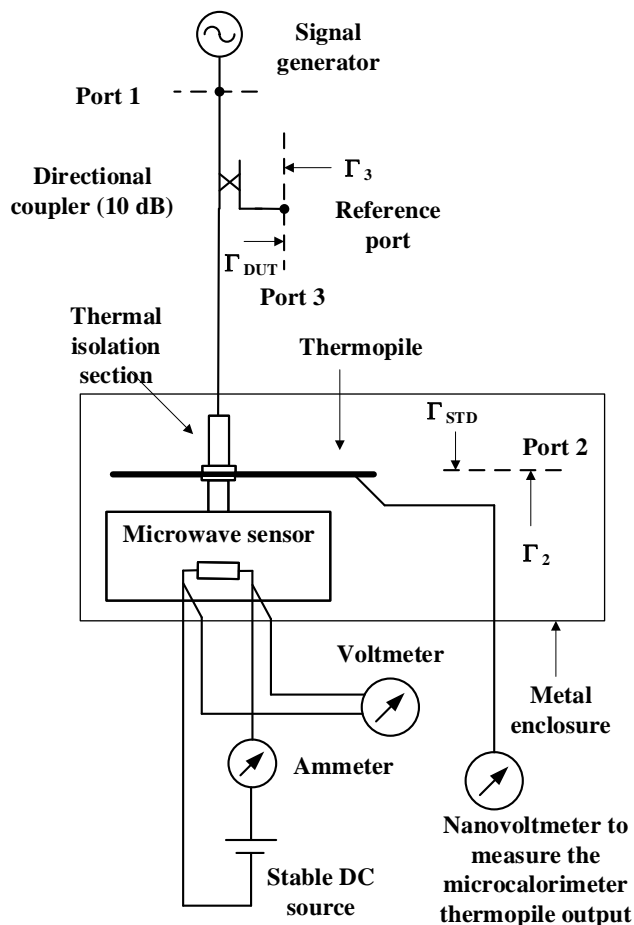


Fig. 1. Block diagram of the National Physical Laboratory's (NPL) waveguide calorimeter from 110 GHz to 170 GHz.

desired frequency and with a specific nominal power level is generated by a signal generator. This signal passes through a directional coupler, where in this case a nominal 10 dB sample of this input signal is coupled onto the reference port whilst the rest passes through the transmission line, the TIS and finally is terminated in the fixed microwave sensor. This fixed microwave sensor can subsequently be used for a DC substitution measurement of the unknown microwave power. The power, whether DC or microwave terminated in the microwave sensor will cause a temperature change on it. In order to measure the temperature change on the terminating microwave sensor due to the dissipated power, a thermopile is located between the TIS and the microwave sensor and is monitored using a nano-voltmeter. The reference side of the thermopile is attached to a dummy sensor which has the same thermal mass as the microwave sensor, TIS and input transmission line which have the same thermal properties as the active side. This is not shown in Fig. 1. This is done to mitigate the thermal effects within the metal enclosure of the calorimeter head caused by ambient temperature variations, thermal leakage or other effects. This is the same technique which would be used for a conventional micro-calorimeter measurement.

The microwave sensor, used to terminate the TIS, contains a multilayer sensor chip with a low-resistivity silicon substrate, which is used as a microwave absorber, and a meander shape platinum thin film DC resistor, which has a positive temperature coefficient. This resistor was used as a heater along with a DC substitution calorimeter technique to characterize the incident microwave power on the calorimeter system. Fig. 2, shows the structure of the microwave sensor. Here, the microwave power is absorbed by the silicon substrate, which raises its temperature. As it is shown in Fig. 2, the chip is sandwiched between two polyimide layers, used for thermal isolation. A silicon dioxide layer (SiO<sub>2</sub>) was used between the silicon substrate and the platinum thin film. This is intended to electrically isolate these two layers from each other. Here, gold plated electrodes are used for electrical connection with the DC biasing circuit through a pair of spring-loaded pin connectors. The platinum thin film is designed to have an electrical resistance of 200 Ω to be compatible with most bridge circuits.

In operation, an unknown microwave CW signal at the

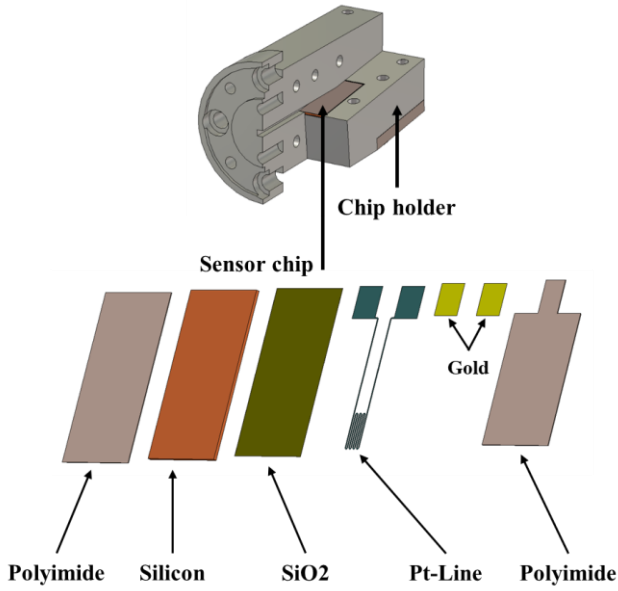


Fig. 2. Structure of the microwave sensor, showing the left half of the waveguide, and the multilayer sensor chip with the layers individually.

Traditionally, the DC substitution technique involves applying a known DC power to the DC resistor and monitoring the thermopile's electromotive force (emf) output. Next, microwave power is applied to the system whilst the DC power is reduced to give the same thermopile emf output. A change in the applied DC power can then be equated to an equivalent change in the dissipated microwave power. This measurement method was not used in this study because of the long stabilization time required for the measurement system. A new method, which relies on the characterization of the thermopile and microwave sensor as a combination using DC power, is proposed here.

#### A. The Thermopile Coefficient

For any given thermopile, there is a relationship between the generated emf voltage on the thermopile ( $e_t$ ) and the temperature difference across it. In this case the difference is between the temperature of the microwave sensor and the reference side ( $\Delta\theta$ ). This is given as  $e_t = \Delta\theta n \varepsilon$ , where  $n$  is the number of thermocouple junctions and  $\varepsilon$  is the Seebeck coefficient (V/K). There is also a linear relationship between the dissipated power ( $P$ ) in the sensor and the temperature change in the sensor which is given as  $P = \Delta\theta k_t A$ , where  $k_t$  is the specific thermal conductivity and  $A$  is the sensor's cross-sectional area. As a result, there is a linear relationship between the dissipated power in the sensor and the thermopile's output emf voltage which can be expressed as:

$$P = \frac{k_t A}{n \varepsilon} e_t. \quad (2)$$

This linear relationship gives the thermopile coefficient ( $c_t$ ) which is defined as:

$$c_t = \frac{k_t A}{n \varepsilon}. \quad (3)$$

A value of this coefficient is valid for an individual thermopile/microwave sensor combination including the mechanical connections of the microwave termination/DC resistor to the sensor housing and therefore to the thermopile. In practice, it is not easy to accurately calculate the thermopile coefficient due to variations in the real calorimeter setups such as the variations in the mechanical connections, which can cause changes in the thermal propagation within the system. It is therefore more convenient to directly measure this thermopile coefficient for each different setup.

#### B. Thermal Isolation Section Heating Effect

In addition to the thermopile heating caused by the dissipated microwave power in the microwave termination, microwave power dissipated in the TIS also generates a small change in the overall system temperature, which affects the observed thermopile emf so this effect should be removed. To determine the effect of the TIS heating, a short foil method was used [11]. An additional measurement with a short foil inserted between the TIS and the terminating microwave sensor was carried out. The short foil is made of the same material as the TIS and has enough thickness to eliminate the skin depth effect. It is assumed for this measurement that the thermal load and the temperature flow within the calorimeter are the same as those for the unknown microwave power measurement. The microwave power at the reference port (port 3) of the directional coupler is also measured as a reference microwave power. The effect of the TIS ( $e_{TIS}$ ) was calculated using the thermopile output ( $e_{short}$ ), the reference port microwave power for the short foil ( $P_R$ ) and for the DUT power sensor ( $P_{DUT}$ ) connections, and the heating ratio of the measurement system ( $HR$ ) as:

$$e_{TIS} = \frac{e_{short} P_{DUT}}{HR P_R}. \quad (4)$$

The heating ratio of the measurement system, which includes the TIS and microwave sensor parameters, was calculated using [11]:

$$HR = \frac{\left\{ \frac{1}{2 A_{TIS}} \left( b + \frac{a}{2} + \frac{\gamma^2 a^3}{2\pi^2} \right) \left\{ (1 + |r_s|^2) l^2 - \frac{2 |r_s| l}{\gamma^2} (\cos(\gamma l + \phi_{r_s})) \right\} + \frac{\gamma^2 a^3 b d}{A_s \pi^2} \right\}}{\frac{1}{2 A_{TIS}} \left( b + \frac{a}{2} + \frac{\gamma^2 a^3}{2\pi^2} \right) \left\{ (1 + |r_{MS}|^2) l^2 - \frac{2 |r_{MS}| l}{\gamma^2} (\cos(\gamma l + \phi_{r_{MS}})) \right\}}. \quad (5)$$

where  $A_{TIS}$  is the cross-sectional area of the TIS's guide walls,  $a$  is the waveguide broad wall width,  $b$  is the narrow wall length,  $\gamma$  is the complex propagation coefficient,  $|r_s|$  is the magnitude and  $\phi_{r_s}$  the phase of the voltage reflection coefficient (VRC) of the short foil,  $A_s$  is the cross-sectional area of the short foil,  $d$  is the thickness of the short foil,  $|r_{MS}|$  is the magnitude and  $\phi_{r_{MS}}$  is the phase of the voltage reflection coefficient of the microwave sensor, and  $l$  is the length of the TIS section.

The dissipated unknown microwave power in the microwave sensor ( $P_{mwd}$ ) can be calculated using the measured thermopile emf ( $e_{tmw}$ ) for the microwave power, as well as the TIS effect

and the known thermopile coefficient with the help of (2), (3) and (4) as:

$$P_{mwd} = (e_{tmw} - e_{TIS})c_t - c_u. \quad (6)$$

where,  $c_u$  is the calorimeter unbalance coefficient.

### C. Microwave Power at the Reference Port

There is a relationship between the incident microwave power on the microwave sensor attached to the port 2 and the power at port 3. The power at the reference port is sampled from the unknown power coming from the signal generator. If the voltage transmission coefficient from the directional coupler's port 1 (connected to the signal generator output) to the reference port (port 3) is defined as  $S_{31}$ , and that from the port 1 to the microwave sensor input (port 2) is defined as  $S_{21}$ , then the ratio between the incident power at the reference port ( $P_{inc}$ ) and the incident microwave power on the microwave sensor ( $P_{mwd}$ ) is obtained using the flow graph method for a 3-port device, is given by (7).

$$\frac{P_{inc}}{P_{mwd}} = \frac{|S_{31}|^2}{|S_{21}|^2} \frac{1-|\Gamma_{DUT}|^2}{1-|\Gamma_{MS}|^2} \frac{|1-\Gamma_2 \Gamma_{MS}|^2}{|1-\Gamma_3 \Gamma_{DUT}|^2}. \quad (7)$$

where  $\Gamma_{MS}$  and  $\Gamma_{DUT}$  are the voltage reflection coefficients of the microwave sensor and of the power sensor or device under test (DUT) connected to port 2 and 3 respectively, and  $\Gamma_2$  and  $\Gamma_3$  are the voltage reflection coefficients of ports 2 and 3 of the system.

If the  $S$ -parameters of the measurement system, the respective reflection coefficients of the microwave sensor and of the DUT power sensor and the absolute microwave power on the microwave sensor are known, then  $P_{inc}$  can be found.

A transfer function for the DUT power sensor can be defined as either an effective efficiency ( $EE$ ) or a calibration factor ( $CF$ ). The effective efficiency is defined as the ratio of the measured power ( $P_{DUT}$ ) as indicated by the DUT, to the known incident microwave power and is given as

$$EE = \frac{P_{DUT}}{P_{inc}} \quad (7)$$

The  $CF$  includes the effect of the effective efficiency and the magnitude of the reflected signal from the DUT's input. The relationship between calibration factor and effective efficiency is  $CF = EE / (1 - |\Gamma_{DUT}|^2)$ .

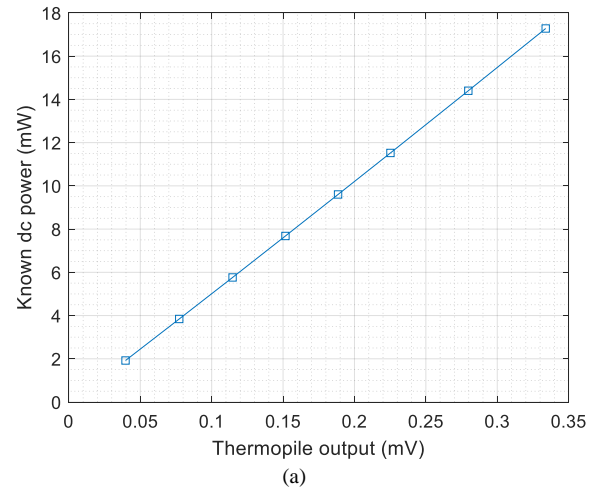
## III. MEASUREMENTS

Measurements to define the incident power on the microwave sensor and the incident power on the DUT were performed in three steps. These were: i) thermopile characterization; ii) microwave power measurement; and iii)  $S$ -parameters measurements. All of these measurements were taken in a controlled laboratory environment at a temperature of  $23 \pm 1$  °C and with sufficient sample sizes to allow for viable statistical analysis of the data.

### A. Thermopile characterization

The calorimeter's thermopile was characterized by using a range of known DC powers generated by a very stable DC source and applied directly to the DC resistor of the microwave sensor using a 4-wire connection (as shown in Fig. 1) in order to cancel out the effect of cables. Measurements from the voltmeter and ammeter (Fig. 1) were used to calculate the exact DC power applied to the microwave sensor. Different nominal DC powers ranging from 2 mW to 17 mW were applied to the DC resistor. These generated different amounts of heating on the sensor and therefore a corresponding change in the thermopile's emf output relative to the applied DC power. As per other measurements with this system, the thermopile emf was measured using the nano-voltmeter.

The applied known DC power and corresponding thermopile output are illustrated in Fig. 3 (a). A linear fit was applied to the data as  $52.194136 \cdot M - 0.202232$  (with  $R^2 = 0.999953$ ), where  $M$  is the measured thermopile output emf in mV. The thermopile coefficient was obtained as  $52.194136 \cdot M$  (mW/mV). The second term shows the calorimeter's unbalance effect ( $c_u = 0.202232$  mW). Additional measurements were performed to verify the thermopile's response. The characterization procedure was then reversed, and the applied DC power calculated using the thermopile output voltage and thermopile's response. The calculated DC, the known DC power as calculated from the measured DC voltage and current, and the difference between them are depicted in Fig. 3 (b).



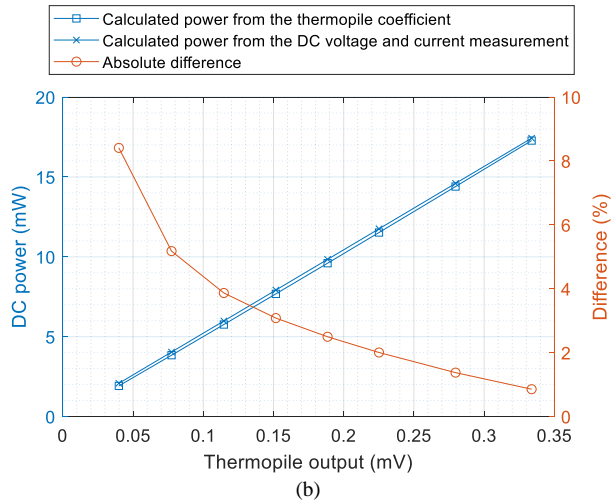


Fig. 3. (a) DC power versus thermopile output. (b) Calculated and measured DC power versus thermopile output voltage and the difference between the DC powers.

The differences between the known and the calculated DC powers across the measured range were between 0.9 % and 8.4 %. This difference shows a trend that is inversely proportional to the thermopile output voltage and becomes increasingly linear when the thermopile output is greater than 0.15 mV. These differences are less than 4.0 % (2.2 % for normal distribution) for thermopile voltages greater than 0.10 mV and around 3.1% (1.8 % for normal distribution) for 0.15 mV corresponding to approximately 6 mW and 8 mW DC powers respectively.

The sensor heating and therefore the thermopile emf, due to the dissipated DC and microwave powers, are not expected to be identical for the same dissipated DC and microwave powers, i.e. there is the skin depth effect. The discrepancy in the detected power is caused by a different current distribution between the DC and the microwave power, and the way in which a change in the temperature at the terminations propagates through the sensor body. To reduce the influence of these effects, the DC resistor used as the DC heater was placed directly on the silicon substrate (microwave absorber) with only a 1  $\mu\text{m}$   $\text{SiO}_2$  layer in between. It is expected that this error is approximately 1.2 % or even lower [12]. As a result, the estimated uncertainty for the calculated microwave power from the thermopile measurements was obtained to be between 0.9 % and 2.3 % for an output voltage greater than 0.10 mV.

### B. Microwave power measurement

As previously mentioned, two measurements were carried out to calculate the microwave power, the first using the short foil inserted between the TIS and the microwave sensor and the second without. The measurement procedure for both was the same except for the setup.

For these measurements, the DC connections to the microwave sensor were removed to eliminate additional temperature leakage from the microwave sensor. A microwave power sensor/meter combination (VDI Erickson PM5 which was also used as a DUT) was connected to the reference port. The output of the power sensor/meter and of the thermopile

were measured, with sample sizes no smaller than 100 with respect to the microwave power OFF and ON for frequencies ranging from 110 GHz to 170 GHz using a prepared script. As with most micro-calorimetry experiments, automation is required as measurements can take days or even weeks to complete.

The ratio of the thermopile output with respect to the measured power at the reference port, for both the foil short and microwave sensor measurements are shown in Fig. 4. The measurement for the microwave sensor is changing from 21  $\mu\text{V}/\text{mW}$  to 46  $\mu\text{V}/\text{mW}$  in the frequency band, and the average thermopile response for the short foil is 14 % relative to the microwave sensor value. The type A standard uncertainties for the microwave sensor measurements obtained were between 0.023 % to 0.065 % with an average of 0.034 %. The type A standard uncertainty for the short foil measurement was lower than 11%.

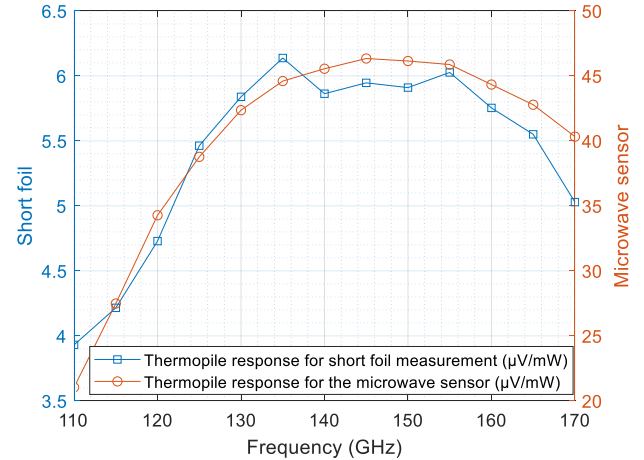


Fig. 4. The thermopile output voltage with respect to the microwave power measured at the reference port for the short foil and microwave sensor measurements.

The dissipated microwave power on the microwave sensor ( $P_{mwa}$ ) was calculated using (6) and the TIS effect ( $e_{TIS}$ ) using (4), the thermopile emf data and the thermopile coefficient. The dissipated microwave power on the microwave sensor and the indicated power on the DUT power sensor attached to the reference port are illustrated in Fig. 5. Calculated incident microwave power on the microwave sensor and DUT power sensor range between 3.3 mW and 16.9 mW, and 3.5 mW and 7.7 mW respectively. Uncertainties were not calculated for (4), (5) and (6) due to the unavailability of traceable, robust uncertainty analysis and budgets for the S-parameter measurements made in this frequency band. Generally, power in between 1 mW and 10 mW is used for the effective efficiency characterization and the power on the DUT power sensor is in this range.

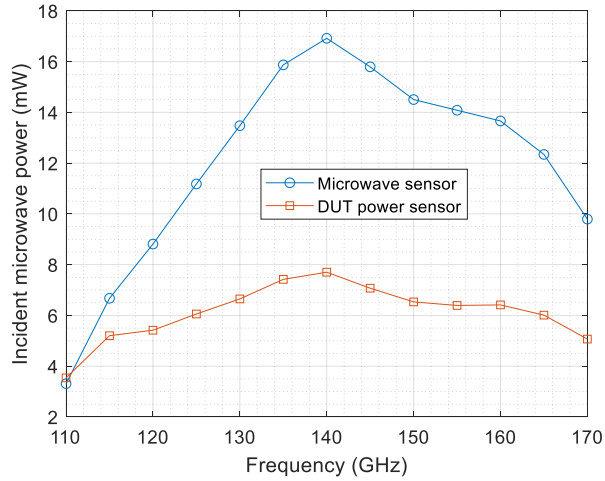


Fig. 5. Incident microwave power on the microwave sensor and on the DUT power sensor.

### C. S-Parameters Measurement

To calculate the power ratio given in (7), the  $S$ -parameters of the measurement system, microwave sensor and DUT power sensor are required. A vector network analyser with WG29 extender heads was used. After performing a through-reflect-line calibration, the complex (real/imaginary)  $S$ -parameters used in (7) were measured and are shown in Fig. 6 and 7.

The nominal specified coupling factor for the directional coupler ( $S_{31}$ ) is 10 dB, whilst the measured coupling factor varied between 8.5 and 9.7 dB with an average of just 9.3 dB. The complex data values for this parameter are shown in Fig. 6 (a). The measured average, maximum and minimum voltage transmission coefficient ( $S_{21}$ ) (Fig. 6 (b)) was calculated as -6.7 dB, -6.1 dB and -8.7 dB respectively. The complex data values for this are shown in Fig. 6. Whilst the minimum return loss for the whole frequency band of port 2 and port 3 was obtained as 23.7 dB, the averages were 30.7 dB and 38.6 dB respectively (Fig. 7)(Fig. 6 (c) and Fig. 6 (d)).

The average return loss of the microwave sensor was measured to be 18.8 dB with a relatively flat response and a standard deviation of 1.8 dB from 110 GHz to 170 GHz (Fig. 6 (e)). The return loss of the DUT power sensor (Fig. 6 (f)) changes from 29.9 dB at 110 GHz to 43.9 dB at 150 GHz. The complex reflection coefficient measurement values are represented in Fig. 7.

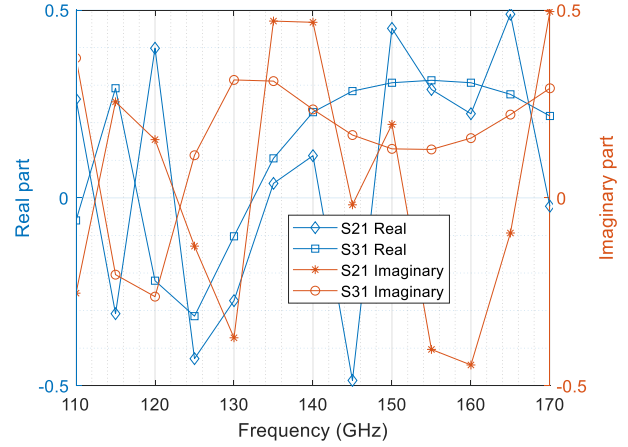


Fig. 6. Measured complex voltage transmission coefficients of the measurement system; directional coupler Port 1 to Port 2 ( $S_{21}$ ) and directional coupler Port 1 to Port 3 ( $S_{31}$ ).

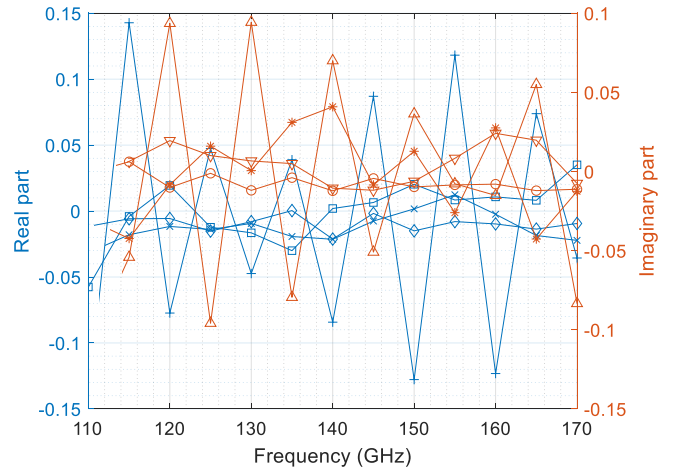


Fig. 7. Measured complex voltage reflection coefficients of the measurement system, microwave termination and DUT power sensor: Real part of  $\Gamma_2$  (—□—), real part of  $\Gamma_3$  (—◇—), real part of  $\Gamma_{MS}$  (—+—), real part of  $\Gamma_{DUT}$  (—×—), imaginary part of the  $\Gamma_2$  (—\*—), imaginary part of  $\Gamma_3$  (—○—), imaginary part of  $\Gamma_{MS}$  (—△—), imaginary part of  $\Gamma_{DUT}$  (—▽—).

### IV. EFFECTIVE EFFICIENCY OF THE DUT POWER SENSOR

Substituting (7) into the definition (1) for the effective efficiency (EE) of the DUT power sensor leads to

$$EE = \frac{P_{DUT} |S_{21}|^2}{P_{mwd} |S_{31}|^2} \frac{1-|\Gamma_{STD}|^2}{1-|\Gamma_{DUT}|^2} \frac{|1-\Gamma_3 \Gamma_{DUT}|^2}{|1-\Gamma_2 \Gamma_{STD}|^2} \quad (8)$$

The calculated EE of the DUT power sensor from 110 GHz to 170 GHz is given in Fig. 8. It varies between 0.9815 at 110 GHz and 0.9386 at 120 GHz, the maximum and minimum observed values. The average EE over the entire frequency range was 0.9592 and has an experimental standard deviation of 0.0096. This variation between the maximum and minimum was likely caused by the applied microwave power level, with

the calculated incident microwave power at 110 GHz, 115 GHz and 120 GHz being 3.3 mW, 6.7 mW and 8.8 mW respectively. According to Fig. 3 (b), these relatively low incident power levels can have a large effect on the observed thermopile output. It is expected that the uncertainty associated with these low power levels will be one dominant factor in the final uncertainty budget for the effective efficiency (which was not calculated as part of this work).

To minimize the error due to the total dissipated power, an additional DC power can be applied to the microwave sensor through the DC resistor together with the microwave power. This generates additional heating on the microwave sensor and therefore additional voltage output from the thermopile, which potentially moves into the linear region of the thermopile at power dissipation levels of greater than 8 mW. The effect of this additional DC power should be removed from the calculated power in order to correctly define the dissipated microwave power.

From the manufacturer's specification for the DUT power sensor (VDI PM5), the accuracy is given as 5 % and the typical losses for the WR 10 waveguide section and for the WR 6 to WR 10 taper are 0.18 dB and 0.17 dB, respectively, in the frequency range from 110 GHz to 170 GHz [13]. A linear correction based on these specifications was calculated as 0.9226 for the whole frequency band. The difference between this linear correction and the measured EE is also depicted in Fig. 8. The absolute differences obtained were between 1.7 % and 6.0 %, and the average over the whole frequency band was 3.8 %.

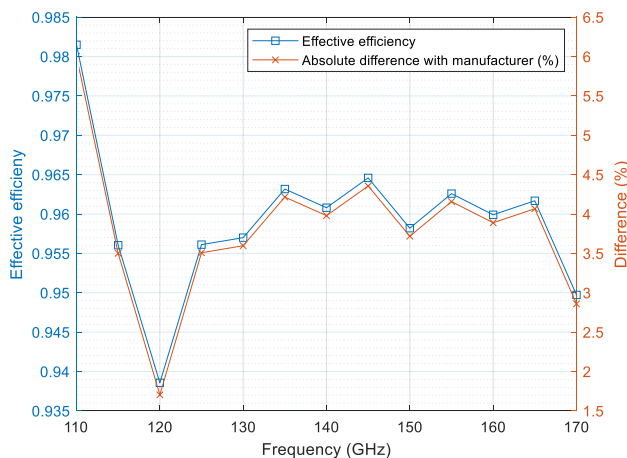


Fig. 8. Calculated DUT effective efficiency (EE) and the difference between the calculated EE and manufacturer's specification.

## V. CONCLUSION

Absolute microwave power was measured using a new technique and a custom-designed microwave sensor in the 110 GHz to 170 GHz frequency range. This was subsequently used to characterize the effective efficiency of a commercial power meter/sensor coupled to the input feed of this system for the given frequency range.

The calorimeter system was characterized using the foil short method, the measurement of the thermopile's response with a range of known DC power levels and the S-parameter measurements of the 3-port calorimeter system. Additional S-parameter measurements of the microwave sensor and of the DUT power sensor allowed for the calculation of the absolute power absorbed by the calorimeter and of the effective efficiency of the DUT. The calculated incident microwave power on the microwave sensor in the WG29 band was between 3.3 mW at 110 GHz and 16.9 mW at 140 GHz.

The calculated effective efficiency for the DUT was compared to that obtained from the manufacturer's specified accuracy and loss of the line section and taper attached to the sensor port. The difference between the calculated and specified effective efficiency was shown to be on average approximately 4 % on average, while the calculated average effective efficiency for the sensor was 0.9592 across the band. The result shows that there is a good agreement between the measurements and the DUT power sensor's specifications.

## ACKNOWLEDGMENT

Authors would like to thank Ian Instone (NPL) for useful discussions during the measurements.

## REFERENCES

- [1] M. L. Crawford and P. A. Hudson, "A Dual-Load Flow Calorimeter for RF Power Measurement to 4 GHz," *Journal of Research of the National Bureau of Standards – C. Engineering and Instrumentation*, vol. 71C, no. 2, pp. 47-54, April – June 1967.
- [2] K. Shimaoka, M. Kinoshita, and T. Inoue, "A broadband waveguide calorimeter in the frequency range from 50 to 110 GHz," *IEEE Trans. Instrum. Meas.*, vol. 62, no. 6, pp. 1828-1833, Jun. 2013, 10.1109/TIM.2012.2225956.
- [3] A. C. Macpherson and D. M. Kerns, "A microwave microcalorimeter", *Rev. Sci. Instrum.*, pp. 27-33, 1955.
- [4] Y. S. E. Abdo and M. Celep, "New effective coaxial twin-load microcalorimeter system," in *2016 Conference on Precision Electromagnetic Measurements (CPEM 2016)*, Ottawa, ON, Canada, 2016, pp. 1-2, doi: 10.1109/CPEM.2016.7540502.
- [5] L. Brunetti, L. Oberto, M. Sellone and E. Vremera, "Comparison among coaxial microcalorimeter models," *IEEE Trans. Instr. Meas.*, vol. 58, no. 4, pp. 1141-1145, April 2009, doi: 10.1109/TIM.2008.2011091.
- [6] E. Vollmer, J. Ruhaak, D. Janik, W. Peinelt, W. Butz and U. Stumper, "Microcalorimetric measurement of the effective efficiency of microwave power sensors comprising thermocouples," in *Proceedings of Conference on Precision Electromagnetic Measurements Digest*, Boulder, CO, USA, 1994, pp. 147-148, doi: 10.1109/CPEM.1994.333409.
- [7] Virginia Diodes, VDI-Erickson power meters (PM5B), <https://www.vadiodes.com/en/products/power-meters-erickson>.
- [8] Elmika, M1-25M/XXE series Calorimetric power meter, [http://elmika.com/calorimetric\\_power\\_meter.html](http://elmika.com/calorimetric_power_meter.html)
- [9] M. Kinoshita, T. Inoue, K. Shimaoka and K. Fujii, "Precise Power Measurement With a Single-Mode Waveguide Calorimeter in the 220–330 GHz Frequency Range," in *IEEE Transactions on Instrumentation and Measurement*, vol. 67, no. 6, pp. 1451-1460, June 2018, doi: 10.1109/TIM.2018.2795878.
- [10] W. Yuan, X. Cui, Y. Li and Y. S. Meng, "Development of a WR-6 Waveguide Microcalorimeter for Thermoelectric Power Sensor," 2018 Conference on Precision Electromagnetic Measurements (CPEM 2018), Paris, France, 2018, pp. 1-2, doi: 10.1109/CPEM.2018.8500864.
- [11] M. Celep and D. Stokes, "Characterization of a Thermal Isolation Section of a Waveguide Microcalorimeter," in *IEEE Transactions on Instrumentation and Measurement*, vol. 70, pp. 1-7, 2021, Art no. 1008007, doi: 10.1109/TIM.2021.3084306.
- [12] Y. Tojima, M. Kinoshita, H. Iida and K. Fujii, "Calibrating Power Meters in the 140–220-GHz Frequency Range Using an Absolute-Power Reference Calorimeter," in *IEEE Transactions on Instrumentation and*



*Measurement*, vol. 70, pp. 1-9, 2021, Art no. 1002709, doi:  
10.1109/TIM.2020.3036083.

[13] Virginia Diodes, PM5 operational manual, 2019.